ELSEVIER

Journal of Nuclear Materials 318 (2003) 300–306

journal of nuclear materials

www.elsevier.com/locate/jnucmat

Microstructural analysis of ion-irradiation-induced hardening in inconel 718

N. Hashimoto *, J.D. Hunn, T.S. Byun, L.K. Mansur

Metals and Ceramics Division, Oak Ridge National Laboratory, P.O. Box 2008, Bldg. 4500S, MS 6136, Oak Ridge, TN 37831-6151, USA

Abstract

As an assessment for a possible accelerator beam line window material for the US Spallation Neutron Source (SNS) target, performance, radiation-induced hardening and microstructural evolution in Inconel 718 were investigated in both solution annealed (SA) and precipitation hardened (PH) conditions. Irradiations were carried out using 3.5 MeV Fe^+, 370 keV He^+ and 180 keV H^+ either singly or simultaneously at 200 °C to simulate the damage and He/H production in the SNS target vessel wall. This resulted in systematic hardening in SA Inconel and gradual net softening in the PH material. TEM microstructural analysis showed the hardening was associated with the formation of small loop and faulted loop structures. Helium-irradiated specimens included more loops and cavities than Fe^+ ion-irradiated specimens. Softening of the PH material was due to dissolution of the γ'/γ'' precipitates. High doses of helium were implanted in order to study the effect of high retention of gaseous transmutation products. Simultaneous with the hardening and/or softening due to the displacement damage cascade, helium filled cavities produced additional hardening at high concentrations.
© 2003 Elsevier Science B.V. All rights reserved.

PACS: 61.72

1. Introduction

In the construction materials surrounding the Spallation Neutron Source (SNS) target, considerable quantities of transmutation products, especially helium and hydrogen, will be generated due to the exposure to a high flux of 1 GeV protons and associated neutrons [1]. Inconel 718 is a candidate material for the SNS accelerator vacuum window and a back-up candidate for the mercury vessel. It is anticipated that atomic displacement rates will be high up to $\approx 10^{-2}$ dpa/s (displacements per atom/second), during the sub-microsecond beam pulse period, with a 60 Hz pulse frequency. The time-averaged displacement rate would be in the range of $\approx 10^{-6}$ dpa/s. The operating temperature is expected to be below 200 °C. Besides the radiation-induced displacement damage, various transmutation products will be generated as a result of nuclear reactions. In particular, hydrogen and helium will be produced at rates of $\approx$1000 and $\approx$100 appm/dpa, respectively.

Hunn et al. [2] have shown that hardening occurs due to ion-induced displacement damage as well as due to the build-up of helium bubbles in ion-irradiated Inconel 718. Fig. 1 compares the percent hardening, relative to an unirradiated specimen, measured by nanoindenter at 150 nm contact depth for specimens irradiated by Fe-ions versus He-ions [2]. Hardening increased as a function of dose and helium concentration. Above a concentration of about 1 at.% He, the hardening in the He-implanted Inconel was measured to be greater than that observed stemming from the Fe-induced displacement damage. In the case of precipitation-hardened (PH) Inconel 718, Fe-irradiation resulted in a systematic

* Corresponding author. Tel.: +1-865 576 2714; fax: +1-865 574 0641/241 3650.

E-mail address: hashimoton@ornl.gov (N. Hashimoto).

0022-3115/03/$ - see front matter © 2003 Elsevier Science B.V. All rights reserved.
doi:10.1016/S0022-3115(03)00013-8

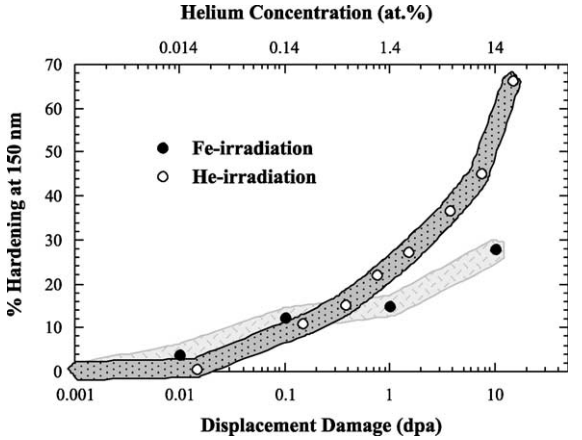

Fig. 1. Percent change in hardness at 150 nm contact depth, relative to unirradiated material, for SA Inconel as a function of dose from Fe-ions and from He-ions [2].

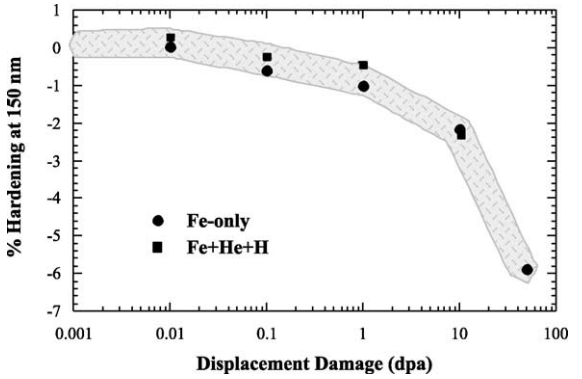

Fig. 2. Percent change in hardness at 150 nm contact depth, relative to unirradiated material, for PH Inconel as a function of Fe-only and from triple-beam irradiation (Fe + He at 200 appm/dpa + H at 1000 appm/dpa) [2].

reduction in the measured hardness at 150 nm contact depth (Fig. 2), while He implantation produced additional hardening in PH Inconel up to a level of 14 at.% He concentration and resulted in partial softening at 20 at.% He concentration (Fig. 3).

In order to better determine the contributions of the different microstructural features on microscopic irradiation-induced hardening and/or softening, SA and PH Inconel 718 irradiated at doses ranging between ~0.01 and ~10 dpa and implanted at ~0.02 and 20 at.% He level were examined by transmission electron microscopy (TEM).

2. Experimental

The nominal composition of the alloy was, in wt%, 53.58 Ni, 18.37 Fe, 18.13 Cr, 4.98 (Nb + Ta), 3.06 Mo,

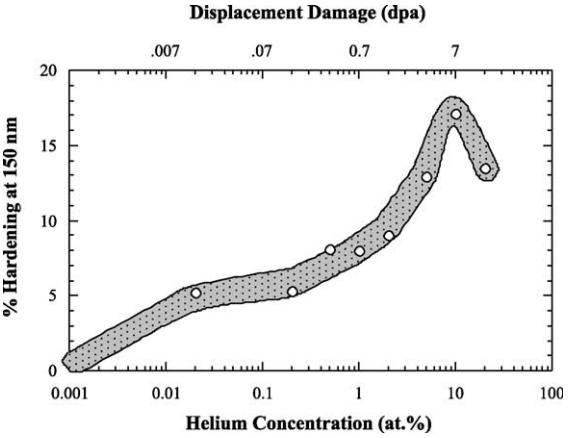

Fig. 3. Percent change in hardness at 150 nm contact depth, relative to unirradiated material, for PH Inconel as a function of helium concentration from He-injection [2].

1.03 Ti, 0.11 Si, 0.48 Al, 0.13 Mn, 0.08 Cu, 0.04 C, 0.001 S, 0.0008 P. Three millimeter diameter and 0.25 millimeter thickness disks were prepared by mechanical and electrochemical polishing prior to irradiation. After final polishing with 0.1 μm diamond paste, specimens were solution annealed (SA) at 1065 °C for 30 min. Some specimens were also hardened by thermal aging at 750 °C for 10 h followed by 650 °C for 20 h. This thermal aging resulted in the formation of γ' and γ'' precipitates. Irradiations were carried out at 200 °C with various combinations of 3.5 MeV Fe^+, 370 keV He^+ and 180 keV H^+ ion beams using the Triple Ion Facility (TIF) at ORNL [3]. The ion energies were chosen for the maximum gas atom deposition and damage to occur near a depth of 825 nm. For the depth calculations, the computer code, Stopping and Range of Ions in Matter (SRIM-2000) was used [4]. The procedure for the dpa calculation is described in [5]. The average concentrations about the 825 nm peak for the He and H injections were calculated as the mean between the two half-maximum points, these numbers were used to calculate the appropriate ion fluencies to give ≈200 appm He/dpa and 1000 appm H/dpa for triple ($Fe^+ + He^+ + H^+$) irradiation and 14 000 appm He/dpa for the He-only irradiation. The initial damage distribution from the Fe-irradiation was calculated in terms of dpa using the NRT formula, using a displacement energy of 40 eV [6]. Damage rates from the Fe-irradiation were from 10^{-4} to 3×10^{-3} dpa/s, with associated gas injection rates of 0.02–0.6 appm He/s and 0.1–3 appm H/s. He-injection rates for the higher concentration He-only implants went as high as 2 appm/s. The SNS will operate with an average dose rate of 10^{-6} dpa/s, in a pulsed mode with a damage flux during the pulse of around 10^{-2} dpa/s and corresponding transmutation rates up to 2 appm He/s and 10 appm H/s. The ion fluxes were lower than the

SNS beam-on rate, however, in this recombination dominant regime of high dose rate and low temperature, we expect irradiation variable shifts [7] to be minimal.

TEM specimens were prepared by electrochemically removing ≈700 nm from the ion bombarded side of the disks and then thinning from the unirradiated side until perforation occurred. This procedure produced TEM foils with thicknesses of ≈100 nm on average and allowed examination of the microstructure at the peak damage region between 700 and 800 nm original depth. Damage microstructure was examined using a JEM-2000FX transmission electron microscope operated at 200 keV. The foil thicknesses were measured by thickness fringes in order to quantify defect density values.

3. Results and discussion

3.1. Microstructural evolution of irradiated SA Inconel 718

Fig. 4 shows the microstructural evolution of SA Inconel 718 as a function of displacement damage from Fe-only and triple-beam irradiation, and from He-ion irradiation. In order to investigate the possible role of trapped gas in the observed hardening, helium was implanted by itself and to higher concentrations. In the cases of the Fe-only and triple irradiation (Fe + He at 200 appm/dpa + H at 1000 appm/dpa) the doses in dpa are shown. In the case of the He ion irradiation the peak helium concentrations are shown. Corresponding dpa production for the He-only irradiation was 0.7 dpa/1 at.%He. The electron micrographs were taken with beam direction **B** close to [0 1 1]. Defect clusters, such as vacancy or interstitial type small loops, Frank type faulted loops, and cavities were examined after the various irradiation levels. Quantitative measurements are given in Table 1. At lower dose levels, small loops only were observed in all irradiation conditions. These images were obtained on the diffraction conditions: $\mathbf{B} \approx [0\,1\,1]$, $\mathbf{g} = 200$, ($\mathbf{g}$, $5\mathbf{g}$). The number densities of small loops in each condition were in the range of 10^{22}–10^{23} m^{-3}. At 0.1 dpa and higher dose levels, Frank type faulted loops were observed on {1 1 1} planes, which were identified by relrod streaks from stacking faults in weak-beam dark-field images. The He-only irradiation induced a slightly higher faulted loop density compared with the other irradiation conditions. Since faulted loops tend to unfault and become perfect loops when the sizes become larger, the actual number density of faulted loops decrease at high dose levels. Cavities were observed in He-ion and triple-beam irradiations at higher dose levels, especially at 2–20 at.% helium. As seen in Fig. 1, irradiation-induced hardening increased as a function of the irradiation dose and helium concentration level, and the hardening in the high dose He-implanted Inconel was measured to be greater than that observed stemming from the Fe-induced displacement damage. The amount of hardening observed for the helium-injected specimens could not be explained by

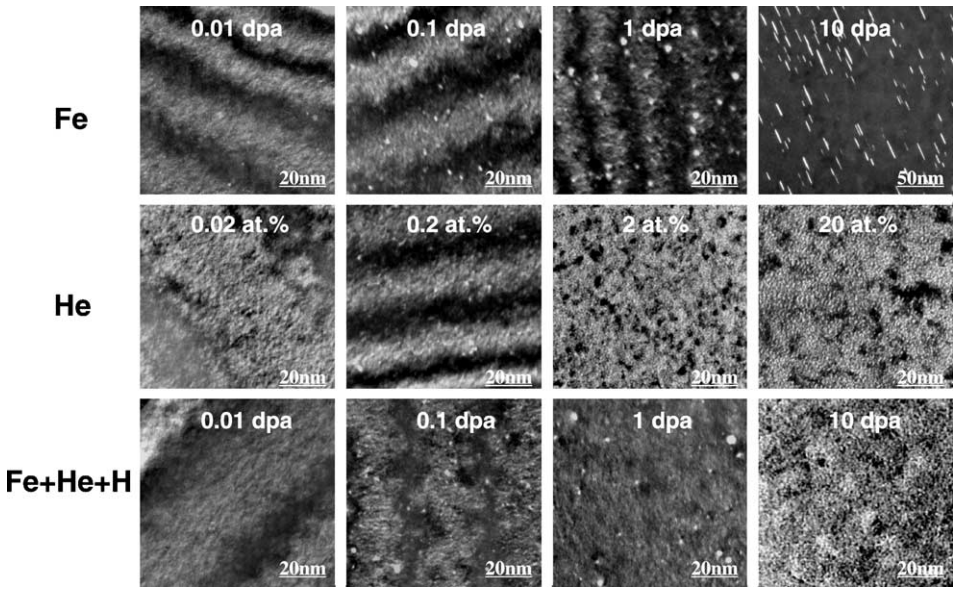

Fig. 4. Microstructural evolution of SA Inconel 718 as a function of dose from Fe-only and triple-beam irradiations, and as a function of implanted helium concentration from He-injection.

Table 1
Summary of number densities and mean sizes of defect cluster, Frank loop and cavities for SA Inconel 718

Irradiation	Dose (dpa)	He (at.%)	H (at.%)	Defect cluster		Frank loop		Cavity	
				Number density (m^{-3})	Mean size (nm)	Number density (m^{-3})	Mean size (nm)	Number density (m^{-3})	Mean size (nm)
Fe^+	0.01			–	–	–	–	–	–
	0.1			7.0×10^{22}	1.1	–	–	–	–
	1			9.0×10^{22}	1.6	–	–	–	–
	10			2.0×10^{23}	<2.0	3.8×10^{22}	20.9	–	–
He^+	0.014	0.02		–	–	–	–	–	–
	0.14	0.2		9.0×10^{22}	1.1	–	–	–	–
	1.4	2		1.0×10^{23}	<2.0	3.0×10^{22}	5.2	3.2×10^{22}	1.0
	7	10		2.0×10^{23}	<2.0	$<1.0 \times 10^{23}$	<20	8.5×10^{22}	1.0
$Fe^+ + He^+ + H^+$	0.01	0.0002	0.001	–	–	–	–	–	–
	0.1	0.002	0.01	8.0×10^{22}	1.2	–	–	1.0×10^{22}	1.0
	1	0.02	0.1	9.0×10^{22}	1.2	–	–	2.0×10^{22}	1.0
	10	0.2	1	2.0×10^{23}	<2.0	2.0×10^{22}	19.3	1.0×10^{23}	1.2

displacement damage alone. This effect was accompanied by the production of observable helium bubbles [8]. Helium bubbles are considered to be a weak barrier for dislocation motion [9]. However, hardness measurement data reported in other work [10] indicated that, when helium bubbles were present in high concentration (above 1 at.%), the barrier strength was augmented as bubbles grew, particularly when helium clusters began to become identifiable as bubbles under TEM.

3.2. Microstructural evolution of irradiated PH Inconel 718

A second set of specimens was prepared in the PH condition by thermal aging as described above. In the unirradiated state, the PH material was considerably harder than its SA counterpart, as expected due to the high density of γ' and γ'' precipitates. Fig. 5 shows the microstructural evolution of PH Inconel 718 as a

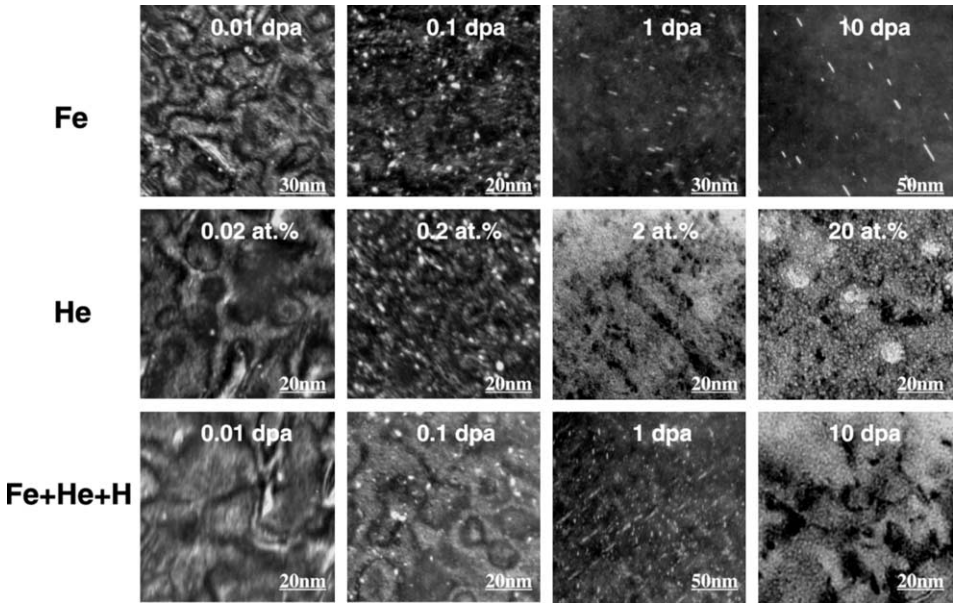

Fig. 5. Microstructural evolution of PH Inconel 718 as a function of dose from Fe-only and triple-beam irradiations, and as a function of implanted helium concentration from He-injection.

Table 2
Summary of number densities and mean sizes of defect cluster, Frank loop and cavities for PH Inconel 718

Irradiation	Dose (dpa)	He (at.%)	H (at.%)	Defect cluster		Frank loop		Cavity	
				Number density (m^{-3})	Mean size (nm)	Number density (m^{-3})	Mean size (nm)	Number density (m^{-3})	Mean size (nm)
Fe^+	0.01			5.5×10^{22}	1.3	–	–	–	–
	0.1			2.3×10^{23}	1.1	–	–	–	–
	1			$<5 \times 10^{23}$	<2	5.0×10^{22}	4.7	–	–
	10			$<5 \times 10^{23}$	<2	9.1×10^{21}	13.6	–	–
He^+	0.014	0.02		3.5×10^{22}	1.1	–	–	–	–
	0.14	0.2		2.3×10^{23}	1.4	–	–	–	–
	1.4	2		$<5 \times 10^{23}$	< 2	1.1×10^{23}	4.1	1.8×10^{23}	1.1
	7	10		$<5 \times 10^{23}$	<2	3.2×10^{22}	8.2	2.8×10^{23}	1.5
$Fe^+ + He^+ + H^+$	0.01	0.0002	0.001	3.0×10^{22}	1.1	–	–	–	–
	0.1	0.002	0.01	1.1×10^{23}	1.4	–	–	–	–
	1	0.02	0.1	$<5 \times 10^{23}$	<2	1.2×10^{22}	3.7	–	–
	10	0.2	1	$<5 \times 10^{23}$	<2	6.5×10^{22}	10.2	1.6×10^{23}	2.3

function of displacement damage from Fe-only and triple-beam irradiation, and as a function of implanted helium concentration from He-injection. Quantitative measurements are given in Table 2. Small loops only were observed at lower dose levels in all irradiation conditions. The number densities of small loops in each condition were in the range of 3×10^{22}–3×10^{23} m^{-3}, which is higher than that in SA Inconel 718. Frank type faulted loops were observed with high number density at $\geqslant 1$ dpa, and some unfaulted loops were present at higher dose level. In the PH Inconel 718 case also, the He-injection induced a slightly higher faulted loop density compared with the other irradiation conditions, and cavities were observed in the specimens irradiated with He-ion and triple-beam at higher dose levels, especially at 2–20 at.% helium concentration level.

The PH Inconel 718, which contains γ' and γ'' precipitates with 10–50 nm size in the matrix, was still harder than the SA Inconel after 10 dpa of irradiation with Fe-ions. However, in contrast to the SA Inconel, displacement damage in the PH Inconel produced a net softening effect (Fig. 2). The triple-beam irradiation showed the same result as for specimens irradiated with Fe-ions alone. Similar softening has been observed in specimens irradiated by 800 MeV protons [11], 1 GeV protons [12] and 5 MeV Ni-ions [13]. Fig. 6 shows the microstructure evolution of γ' and γ'' precipitates with associated diffraction spots as a function of displacement damage from Fe-only irradiation. These images were obtained on the diffraction conditions: $\mathbf{B} \approx [0\,0\,1]$. As seen in Fig. 6, the γ' and γ'' superlattice diffraction spots observed in the unirradiated sample

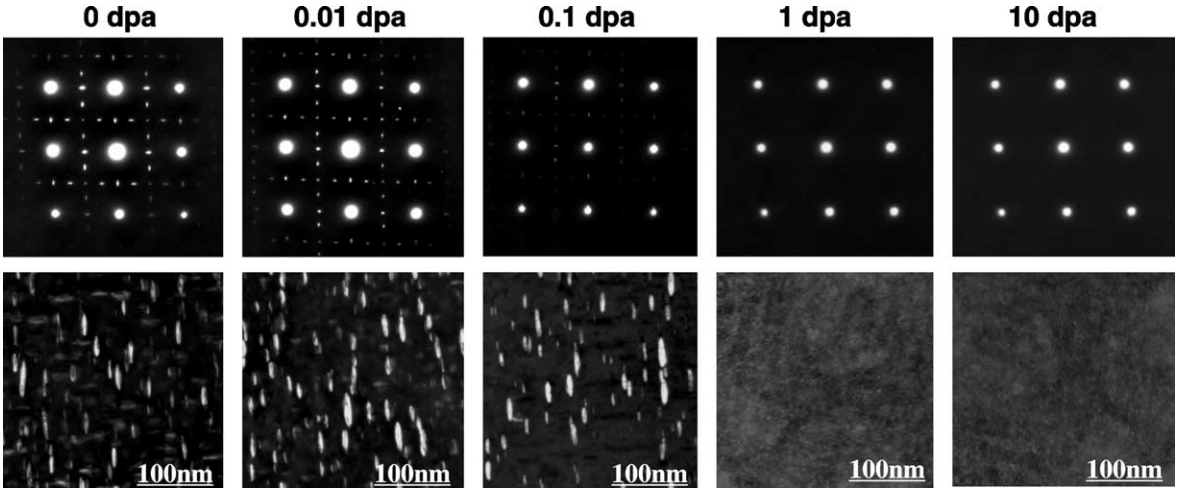

Fig. 6. Microstructure evolution of γ' and γ'' precipitates with associated diffraction spots as a function of dose from Fe-only irradiation.

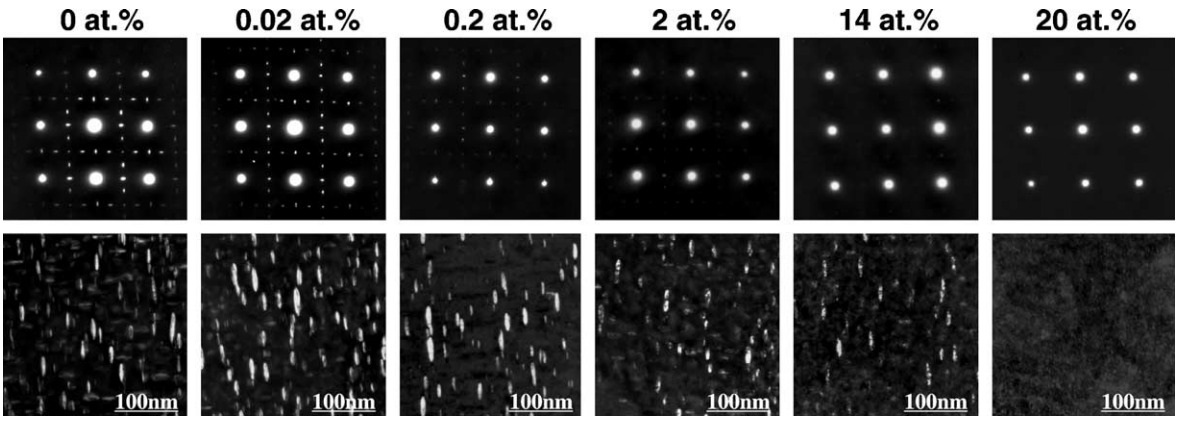

Fig. 7. Microstructures and diffraction patterns as a function of helium concentration for He-implanted PH Inconel 718.

were gone by 1 dpa. This indicates the cause of softening to be the loss of coherency of the γ' and γ'' precipitates, in agreement with findings from 800 MeV proton irradiations [11,14]. Even though the Fe-ion irradiation also introduced radiation defects, the loss of the precipitates outweighed the hardening contribution from these defects. Fig. 7 shows the microstructures and diffraction patterns as a function of helium concentration for He-implanted PH Inconel 718. By 0.2 at.%, the precipitates had begun to disappear and their diffraction spots became less intense. At 14 at.%, the diffraction spots for γ' and γ'' precipitates were almost gone, although some residual contrast still remained in the dark field images. This may suggest that a structural homogenization was occurring while a compositional inhomogeneity between the matrix and post-precipitate zones still persisted. By 20 at.%, there was no further evidence of the precipitates. The specimen implanted with 20 at.% helium showed no rings in the diffraction patterns associated with the break-up of the precipitates. This indicates that the γ' and γ'' precipitates did not become amorphous, but rather they dissolved back to into solution. As shown in Fig. 3, a net hardening as a function of helium concentration was observed by 14 at.% helium concentration, and at 20 at.% He, which corresponded to 14 dpa, some softening was evident. This shows that the build-up of helium in the lattice and its associated deformation pinning occurred at a greater rate than the disordering of the γ' and γ'' precipitates until 14 at.% helium concentration level. The 20 at.% helium implantation resulted in some reversal of the hardening due to the dissolution of the γ' and γ'' precipitates.

4. Conclusions

Ion-irradiation-induced hardening in Inconel 718, both in the SA and the PH condition, has been examined by using nanoindentation technique and TEM.

4.1. SA Inconel 718

At lower dose levels, only small loops were observed at all irradiation conditions. The irradiation condition did not strongly affect small loop nucleation. Frank type faulted loops were observed at higher dose levels. The He-injection induced a slightly higher faulted loop density compared with the other irradiation conditions. Cavities were observed in the specimens irradiated with He-ions and triple-beams at high dose levels. Irradiation-induced hardening increased as a function of irradiation dose and helium concentration. The larger amount of hardening observed for the helium-injected specimens would be due to helium bubble formation, which act as greater barriers to dislocation motion than the small loops and faulted loops.

4.2. PH Inconel 718

The number densities of small loops were higher than observed in SA Inconel 718 as a function of dose. The He-injection induced a slightly higher faulted loop density compared with the other irradiation conditions, and cavities were observed in the specimens irradiated with He-ions and triple-beams at higher dose levels. In the Fe-irradiated sample, the γ' and γ'' superlattice diffraction spots were gone by 1 dpa, indicating the cause of softening to be the loss of coherency of the γ' and γ'' precipitates. Even though the Fe-ion irradiation also introduced radiation defects, the loss of the precipitates outweighed the hardening contribution from these defects. In the He-ion irradiated material a net hardening as a function of helium concentration was observed up to 14 at.% helium concentration, and some softening was evident at 20at.% He. This shows that the deformation pinning was affected at a greater rate by the build-up of helium in the lattice than by the disordering of the γ' and γ'' precipitates up to 14 at.% helium. The 20 at.% helium implantation resulted in some loss of the

hardening due to the dissolution of the γ' and γ'' precipitates.

Acknowledgements

This research was sponsored by the Division of Material Science and Engineering, US Department of Energy, under contract No. DE-AC05-00OR22725 with UT-Battelle, LLC.

References

[1] L.K. Mansur, T.A. Gabriel, J.R. Haines, D.C. Lousteau, J. Nucl. Mater. 296 (2001) 1.
[2] J.D. Hunn, E.H. Lee, T.S. Byun, L.K. Mansur, J. Nucl. Mater. 296 (2001) 203.
[3] M.B. Lewis, W.R. Allen, R.A. Buhl, N.H. Packan, S.W. Cook, L.K. Mansur, Nucl. Instrum. and Meth. B 43 (1989) 243.
[4] J.F. Ziegler, J.P. Biersack, U. Littmark, The Stopping and Ranges of Ions in Solids, Pergamon, New York, 1985.
[5] E.H. Lee, Nucl. Instrum. and Meth. B 151 (1999) 29.
[6] M.J. Norgett, M.T. Robinson, I.M. Torrens, Nucl. Eng. Des. 33 (1975) 50.
[7] L.K. Mansur, J. Nucl. Mater. 216 (1994) 97.
[8] E.H. Lee, J.D. Hunn, T.S. Byun, L.K. Mansur, J. Nucl. Mater. 280 (2000) 18.
[9] S.M. Bruemmer, J.I. Cole, R.D. Carter, G.S. Was, Mater. Res. Soc. Symp. Proc. 439 (1997) 437.
[10] E. Camus, in: Proceedings of the Second International Workshop on Spallation Materials Technology, Ancona, Italy, 19–22 September 1997, p. 445.
[11] F. Carsughi, H. Derz, P. Ferguson, G. Pott, W. Sommer, H. Ullmaier, J. Nucl. Mater. 264 (1999) 78.
[12] S.A. Maloy, M.R. James, G.J. Willcutt, W.F. Sommer, W.R. Johnson, M.R. Louthan Jr., M.L. Hamilton, F.A. Garner, in: S.T. Rosinski, M.L. Grossbec, T.R. Allen, A.S. Kumar (Eds.), Effects of Radiation on Materials, 20th International Symposium, ASTM STP 1405, American Society for Testing and materials, West Conshohocken, PA, 2001.
[13] W.L. Bell, T. Lauritzen, E.S. Darlin, R.W. Warner, in: Irradiation Effects on the Microstructure and Properties of metals, ASTM STP 611, American Society of Testing and Materials, 1976, p. 353.
[14] B.H. Sencer, G.M. Bond, F.A Garner, M.L. Hamilton, B.H. Oliver, L.E. Thomas, S.A. Maloy, W.F. Sommer, M.R. James, P.D. Ferguson, J. Nucl. Mater. 283–287 (2000) 324.